R. E. Link, J. D. Landes†, R. Herrera‡, and Z. Zhou†*

Something New on Size and Constraint Effects for *J–R* Curves

REFERENCE Link, R. E., Landes, J. D., Herrera, R., and Zhou, Z., **Something new on size and constraint effects for *J–R* curves**, *Defect Assessment in Components – Fundamentals and Applications*, ESIS/EGF9 (Edited by J. G. Blauel and K.-H. Schwalbe) 1991, Mechanical Engineering Publications, London, pp. 707–721.

ABSTRACT The effect of specimen size on the *J–R* curve was in the past solved to the satisfaction of many people. Recent test results have revealed some problems with these previous solutions; these are due to two new practices. First, the previous *J–R* curves were strictly controlled in the extent of crack extension to initial uncracked ligament, $\Delta a/b_0$, for the test. In an attempt to develop more *J–R* curve, particularly with a smaller specimen, previous limits are now being disregarded and the $\Delta a/b_0$ range of the test is increased by factors of 2–4. Second it was discovered that previously size effects were sometimes related to experimental technique and data analysis and were actually artefacts of the test method. A new method of data analysis based on normalisation principles can eliminate these artefacts and gives a new perspective on size effects in *J–R* curves.

In this work the method of normalisation is used to develop *J–R* curves for test results from five different materials, in tests which largely excluded fracture mode transition effects. For each of these materials a number of specimens of different sizes and thicknesses were tested to explore both the effects of size and constraint.

The results show that *J–R* curve size effects are not generally observed in any consistent trend. The study of geometry effects shows a gradual increase in the *R* curve as the loading mode changes from predominately bending to pure tension. The effect of constraint continues to be undefinable. Traditionally toughness was observed to increase as constraint (thickness) decreased. However, new results show toughness decreasing with decreasing constraint on some of the more ductile materials.

Introduction

In order to predict accurately the crack growth behaviour in structures, due consideration must be given to all of those factors which may influence the fracture performance of the structure. A fracture assessment consists of analysis of two elements: the deformation response of the structure, the relationships which define the behaviour such as $P = P(a, v)$ and $J = J(P, a)$ and the fracture resistance, typically expressed as a resistance curve or *J–R* curve, $J = J(\Delta a)$ **(1)(2)**. When assessing a cracked structure from a safety standpoint, a lower bound *J–R* curve is often used to define the fracture resistance in a suitably conservative manner. In order to measure a lower bound fracture toughness, it is first necessary to understand how various factors can influence the measured *J–R* curve. Three areas that can influence the measured fracture toughness and that have received the most attention are specimen size, geometry and constraint **(3)**. For the purposes of this paper the

* David Taylor Research Centre, Annapolis, Maryland, USA.
† University of Tennessee, Knoxville, Tennessee, USA.
‡ National University of Mar Del Plata, Mar Del Plata, Argentina.

following definitions of size, geometry, and constraint will be used. Size refers to the overall dimensions of the specimen; changes in size are considered to be a proportional change in both planar and thickness dimensions of a specimen or structure. Geometry refers to the shape of the specimen as well as loading mode, i.e., tension, bending or some combination of tension and bending. Constraint refers to changes in the thickness dimension of the specimen which can vary from a thick highly constrained state (plane strain) to a thin, unconstrained condition (plane stress).

The effect of specimen size on the J–R curve was solved to the satisfaction of many people in the past **(3)(4)**. Recent test results have revealed some problems with these previous solutions; these are due to two new practices. First, the previous J–R curves were strictly controlled in the extent of crack extension permitted relative to the initial remaining ligament, $\Delta a/b_0$, for the test **(5)(6)**. In an attempt to develop more J–R curve, particularly with a smaller specimen, previous limits are now being disregarded and the $\Delta a/b_0$ range of the test is being increased by factors of 2–4 **(7)**. Second, it was discovered that, previously, size effects were sometimes related to experimental technique and data analysis and were actually artefacts of the test method **(8)**. A new method of data analysis based on normalisation principles can eliminate these artefacts and give a new perspective on size effects in J–R curves **(9)(10)**.

Geometry effects have also been examined in the past by several researchers **(3)(11)(12)**. These studies concluded that geometry independent J–R curves for several bending and tension specimen geometries could be obtained by using the modified J integral, J_M, to characterise the fracture toughness **(13)**. This was somewhat in contrast to analysis of crack tip fields which showed that much larger specimens are needed to ensure J controlled crack growth in tension versus bending **(14)**. Re-analysis of these results using normalisation techniques changed this conclusion somewhat.

The broad topic of constraint and its effects on fracture toughness, especially in the transition regime, has received much attention but remains unresolved at this time **(11)**. From a mechanistic viewpoint, the general trends resulting from changes in constraint are thought to be understood. As the constraint changes from plane strain to plane stress, this loss of constraint leads to an increase in the fracture toughness. This idea formed part of the rationale for thickness requirements in J_{IC} and J–R curve testing. A minimum thickness was required in order to ensure that a lower bound fracture toughness was being measured. The results of this study indicate that this is not always the case and that consideration of other factors such as the micromechanisms of the fracture process must be considered as well.

In this paper test results from five different steels are used to study the effects of size, geometry, and constraint on J–R curve fracture toughness. In some cases results have already been reported from tests analysed by the elastic compliance method of crack length monitoring. These results were re-analysed using the normalisation procedure. The re-analysed results along

Table 1 Mechanical properties of steels investigated

Material	*0.2% yield strength MPA (ksi)*	*Tensile strength (ksi)*	*Reduction in area (%)*	*Elongation in 50 mm (2 in)*
A508	386 (56)	545 (79)	60	28
A533B	469 (68)	620 (90)	58	22
A736	470 (68)	565 (82)	76	30
5NiCrMoV	972 (141)	1034 (150)	62	20
304 SS	294 (24.6)	611 (88.6)	80	76

with the new ones give some different conclusions regarding effects on J–R curves, especially the effect of constraint.

Materials

Five different steels, covering a variety of strength levels were used in this study. Since some of the data used in this study were obtained from previous studies reported in the literature, data were not always available to address all issues (size geometry and constraint) on each steel. The steels used in this study were an A508, Class 2A steel from a 21 in. thick forged plate **(3)(11)**; an A533B, Class 1 steel from a 10 1/2 in. thick forging but machined to 0.1 in. thickness **(3)(11)**; an A736 steel from a 5 in. thick plate; a 5NiCrMoV steel from a 4 in. thick plate; and a 304 stainless steel **(15)**. The mechanical properties of these steels are given in Table 1.

Analysis procedure

In this work, the method of normalisation is used to develop J–R curves from the load–displacement test records. Following Ernst *et al.* **(16)**, it is assumed that for fixed proportions between overall specimen dimensions the relationship between load, P, displacement, v, and crack length, a, can be expressed as the product of two separable, multiplicative functions

$$P = G(a/W)H(v_{pl}/W) \tag{1}$$

where W is the specimen width and v_{pl} is the plastic component of displacement. The total displacement is separated into its elastic and plastic components using the equation

$$v = v_{el} + v_{pl} \tag{2}$$

where the elastic displacement is related to the load by the compliance, C, which is a function of the crack length

$$v_{el} = PC(a/W) \tag{3}$$

If functional relationships for G, H and C can be found, then it is possible to determine uniquely the crack length and hence, crack extension, for any given load–displacement pair.

Equation (1) can be recast in the following form

$$P_N = P/G(a/W) = H(v_{pl}/W) \tag{4}$$

where P_N is a normalised load which is a function H of material properties alone. The normalising function $G(a/W)$ can be written in a more convenient format for various geometrical configurations. For example, Ernst showed that for edge cracked geometries with primarily bend type loading, $G(a/W)$ could be given as

$$G(a/W) = \{b^2 B g(b/W)\}/W \tag{5}$$

where the remaining ligament, $b = (W - a)$, and $g(b/W)$ is a function of the specimen geometry and B is the specimen thickness. For the compact specimen, $g(b/W)$ is given by $\exp(0.522b/W)$ and is equal to 1 for the three point loaded bend specimen.

By plotting P_N versus v_{pl}/W, the functional relationship between P_N and $H(v_{pl}/W)$ can be established graphically. When the functional form of H is defined, a relationship exists between P, v, and a from which any one parameter can be determined given the other two. The initial work on this method **(9)(17)** used experimental results from tests of blunt notched specimens and finite element analyses to suggest that for materials whose constitutive behaviour can be modelled by a power law expression, the relationship for H could also be expressed as a power law

$$v_{pl}/W = \beta P_N^n \tag{6}$$

where n and β are constants. This expression is similar to the one chosen by Joyce and Hackett for calculating J–R curves for dynamically loaded specimens **(18)**. Equations (3) through (6) can be combined and arranged to yield the following expression containing the unknown constants β and n

$$v = PC(a/W) + \beta W[PW/\{Bb^2 g(b/W)\}]^n \tag{7}$$

The constants can be determined by considering any two points where the three quantities, P, v, and a are known. One convenient point is the final point from the test where the final measured crack length corresponds to the last recorded load–displacement pair. A second point can be selected from anywhere along the load–displacement record prior to crack initiation when the initial crack length is also known from post test measurements. Alternatively, many points prior to crack initiation together with the final crack size can be used to determine a set of constants which best matches equation (7) with the experimental data. Once the constants have been determined, the crack length and crack extension can be determined for all other load–displacement pairs between the initial and final crack sizes. Given the complete set of load, displacement, and crack length data, the value of J can be determined at every point in the test record using approximate formulations given in ASTM Standard Test Method E1152 or a more direct expression can be developed using

the expression **(19)**

$$J = K^2(1 - \nu^2)/E + \frac{\eta_{pl}}{Bb}\int_0^{v_{pl}} P \, dv_{pl} \tag{8}$$

Additional work on the method of normalisation showed that the power law assumption of material deformation was not suitable for all materials **(10)(20)**. In particular those materials that exhibited extensive deformation before the fracture process begins have a deformation pattern which combines a power law and straight line for load versus plastic displacement. This behvaiour can be modelled analytically by using a more complicated functional relationship, one that has three fitting constants rather than the two needed by the power law. A description of this approach is given in reference **(20)**.

Size effects

In order to investigate the effect of size on J–R curves, compact speciments, C(T), were tested for a variety of specimen sizes. The materials used in the size study were A508 steel with C(T) specimens with sizes of 1/2T, 1T, 4T and 10T; A736 steel with specimens from 1T, 2T and 5T; and 5NiCrMoV using 1T, 2T and 4T specimens. All specimens were precracked in fatigue before testing; tests were conducted at temperatures well above the fracture mode transition temperature. Figure 1 shows the specimen geometry and relevant dimensions of the various compact specimen sizes. Whenever thickness is proportional to planar dimensions ($W = 2B$), it is not given separately. When thickness is

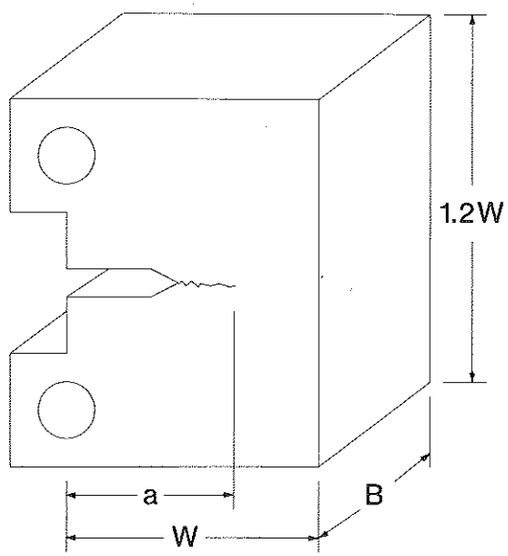

SIZE	W
10T	508 (20)
5T	254 (10)
4T	203 (8)
2T	102 (4)
1T	51 (2)
1/2T	25 (1)

Dimensions are in mm (in.)

For proportional specimens, B=W/2

Fig 1 Dimensions of compact specimens used in the size study

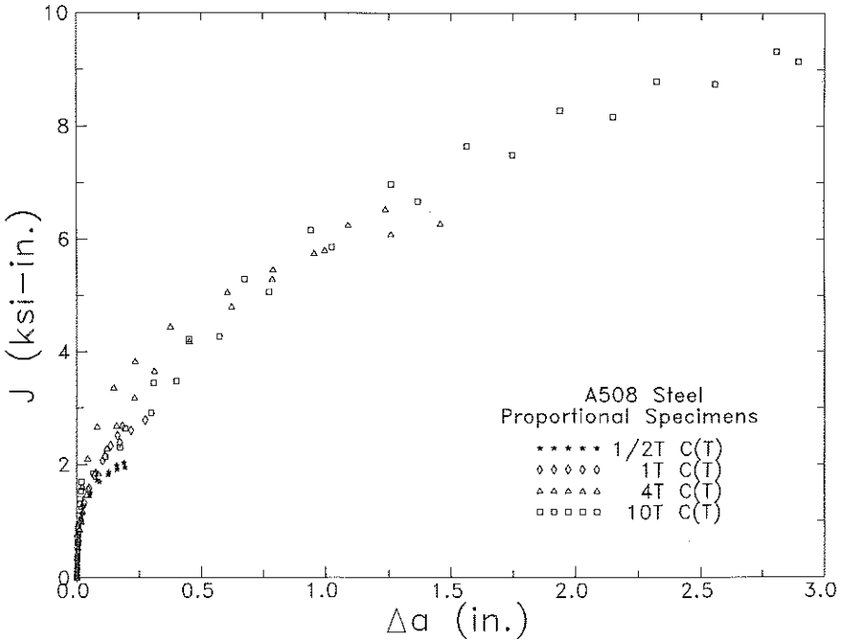

Fig 2 *J–R* curve for A508 steel looking at the effect of specimen size

specified separately, it is not proportional to planar dimensions. The *J–R* curves were calculated using the normalisation method and the results are plotted in Figs 2–4. A consistent resistance curve (within normal material scatter) was observed over the full range of specimen sizes for each material examined. In all cases, no systematic effect of specimen size was noted, even when the crack extension exceeded the 0.1 b_0 limit imposed by ASTM E1152. Other researchers have used the modified J integral, J_M, in order to eliminate apparent size effects in resistance curves **(3)(11)(13)**. This was not found to be necessary for these materials, on the contrary, the use of J_M in some cases produced a size effect. The *J–R* curves for the A736 steel show no size effect; however, when plotted as a J_M–R curve the smaller specimens give unconservatively high toughness results, Fig. 5.

Geometry effects

In order to study the effect of geometry on *J–R* curves, data from an earlier study **(3)(11)** on geometry effects was re-examined using the normalisation method to calculate the resistance curves. The available data were from tests on A533B, Class 2 steel. Specimens which generated a wide range of loading modes from predominantly bending in the compact tension specimen (the bending to tension ratio, $\sigma_B/\sigma_T \approx 10$) to pure tension in the centre-cracked

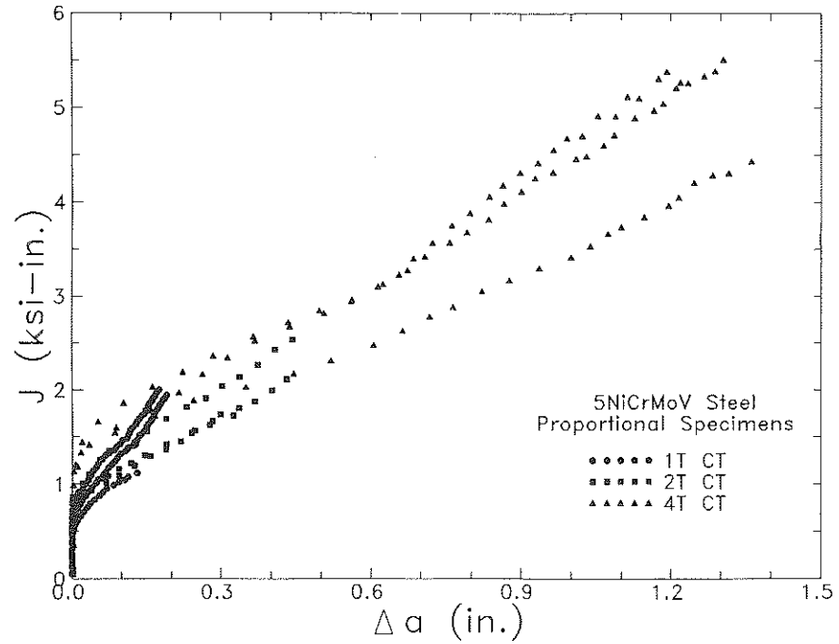

Fig 3 *J–R* curve for A736 steel looking at the effect of specimen size

tension, CCT, and double-edge notched tension, DEN(T), specimens were used. Intermediate ratios of bending to tension were achieved by varying the initial crack length in single-edge notch tension specimens, SEN(T). The SEN(T) specimen provided a $\sigma_B/\sigma_T = 1.3$ for $a/W = 0.3$ to $\sigma_B/\sigma_T = 7.0$ for $a/W = 0.7$. All specimens were machined to a thickness of 2.5 mm in order to generate a predominantly plane stress constraint condition. Specimen geometries are shown in Fig. 6. In addition to the use of the normalisation method, η_{pl} factors were determined for several of the specimen geometries using a new technique developed by Sharobeam and Landes **(21)**, which uses the load separation property **(16)** to develop η_{pl} factors which are more accurate than previously used ones.

The resistance curves determined from the re-evaluated results *et al.* are plotted in Fig. 7. This figure shows that the predominantly bend type loading produces the lowest *J–R* curve, with both the C(T) and deeply cracked SEN(T) producing similar results. The *J–R* curves show an increase in toughness as the σ_B/σ_T ratio decreases. Both of the pure tension geometries yielded *J–R* curves which were substantially higher than those from the bend geometries. The CCT specimen yielded a slightly higher *J–R* curve than the DEN(T) specimen. These results are different from those previously reported **(11)**, where it was shown that J_M collapsed all but the CCT curves to a single *J–R* curve. There are several reasons to account for the different results, including a new

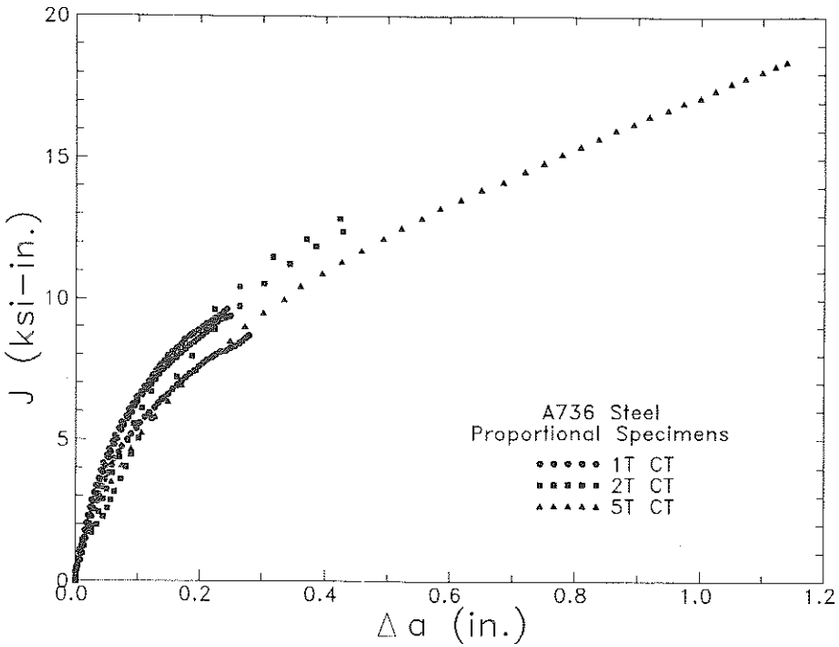

Fig 4 *J–R* curve for 5NiCrMoV steel looking at the effect of specimen size

elastic compliance function and the new η_{pl} values. The current results make sense qualitatively if one considers the crack tip fields associated with each of the specimen geometries indicated schematically in Fig. 6. Numerical studies by McMeeking and Parks showed that it is more difficult to achieve an HRR type of stress singularity for purely tension loading as compared with predominately bend type of loading **(14)**. The effect appears here as an elevation in the *J–R* curve. This elevation is progressively approached as the bending component of loading decreases relative to the tension component.

Geometry effects are sometimes studied using the modified J, J_M–R curve. Figure 8 plots the J_M–R curve for the data from Fig. 7. The result is that the C(T) specimen toughness is elevated and the three other specimens show little change in toughness. Using J_M does not help to resolve differences observed between bend and tension modes of loading. These differences may result from differences in crack tip field which must be acknowledged in using *J–R* curve toughness for structural analysis. The C(T) results give a lower bound *J–R* curve here but not a lower bound J_M–R curve.

Constraint effects

The effects of changes in constraint due to changes in specimen thickness were studied on A508 steel, A736 steel, 5NiCrMoV steel, and 304 stainless steel. 2T

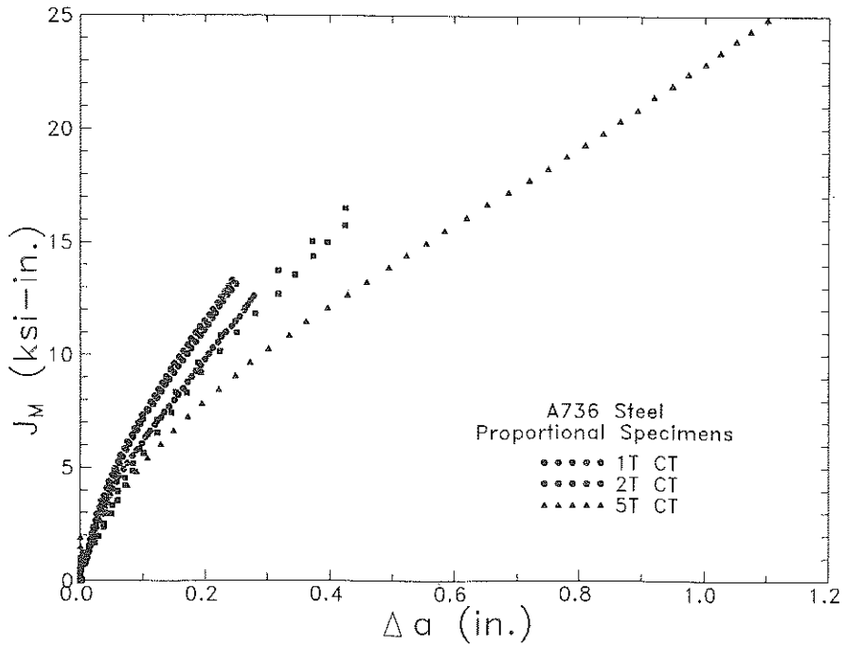

Fig 5 J_M–R curve for A736 steel

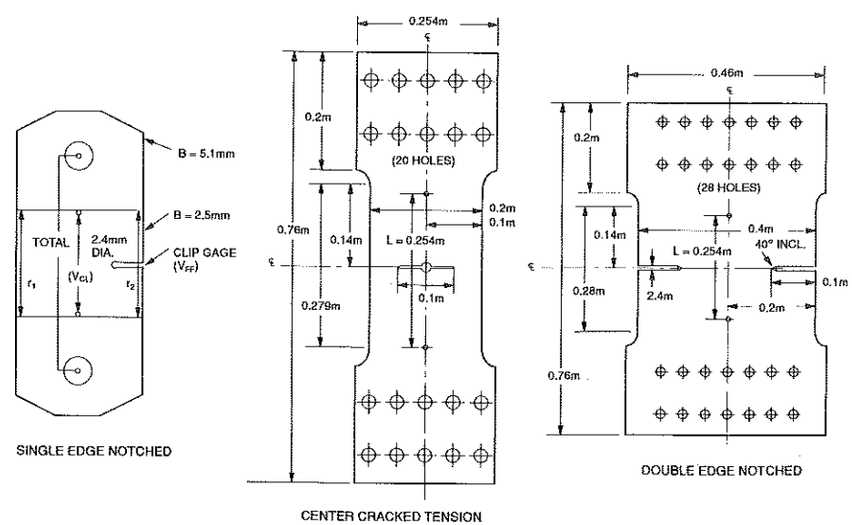

Fig 6 Specimen geometries used in the geometry effect study

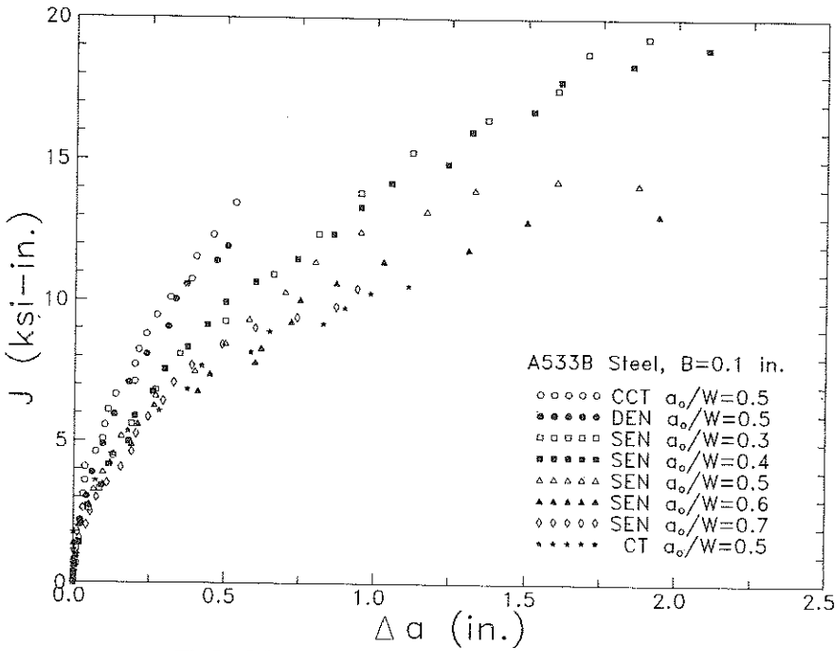

Fig 7 *J–R* **curve for A533B steel for different geometries**

C(T) specimens of A736 and 5NiCrMoV steel were tested in thicknesses ranging of 6.4 mm (0.25 in.) to 51 mm (2 in.). A508 steel was tested in thicknesses ranging from 12.7 mm (0.5 in.) to 102 mm (4 in.) and 304 stainless steel was tested in thicknesses ranging from 12.7 mm (0.5 in.) to 51 mm (2 in.).

In general, it was believed that as constraint changes from plane strain to plane stress, the lowering of constraint leads to an increase in the fracture resistance of a material. This trend was observed for both the A508 steel and the 5NiCrMoV steel as shown by the *J–R* curves plotted in Figs 9 and 10, respectively. Reducing the thickness led to a rise in the measured fracture toughness in the region of slow, stable tearing.

A somewhat surprising result was observed when similar tests were conducted on 304 stainless steel, (Fig. 11) and A736 steel (Fig. 12).

The 304 stainless steel shows almost no change in the *J–R* curve with decreasing thickness, however, at the larger crack extensions the *R* curve appears to have a lower trend in the thin specimen. The *J–R* curve for the A736 steel shows a clear decrease in toughness with decrease in thickness. Here the decrease is progressive. As the thickness changes form 51 mm (2.0 in.) to 12.8 mm (0.5 in.) the toughness begins to decrease slightly. However, with a decrease in thickness to 6.4 mm (0.25 in.) the toughness is clearly lower.

This systematic decrease in toughness with decrease in thickness is somewhat unexpected in that it is contrary to most previously reported results.

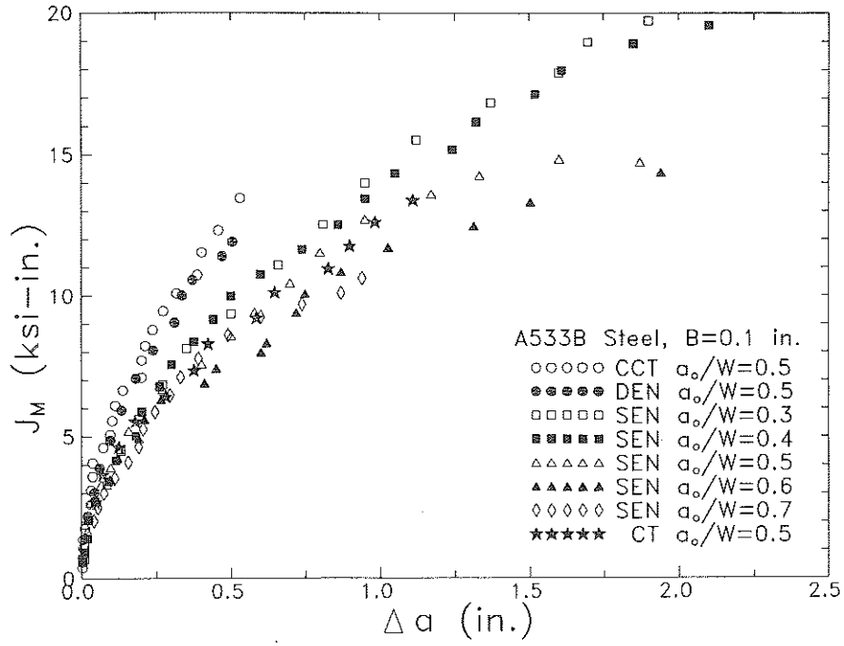

Fig 8 J_M**–***R* **curve for A533B steel four different geometries**

However, both the 304 stainless steel and A736 steel are very ductile materials. A systematic study of microstructural causes was beyond the scope of this work. However, it is likely that the effects of reduced constraint on toughness would be related to the microscopic process of ductile fracture. Since ductile fracture is a process related to the nucleation, growth, and coalescence of voids, the less ductile materials which have many sites for void nucleation can undergo a ductile fracture process easier under high constraint. Lowering constraint could cause increased difficulty with the process of void nucleation.

On the other hand, the very ductile materials have fewer void nucleation sites and may find the ductile fracture process easier with lower constraint. The fracture process in low constraint would likely be related to an out-of-plane or through-thickness deformation process. With increasing constraint the ductile fracture process is easier when a good number of void nucleating sites exist but is more difficult when these sites are not so available.

The apparent conflict observed for effect of constraint suggests that it may be difficult to ensure a conservative lower bound toughness level. Certainly requiring that a specimen has sufficient thickness may not guarantee a lower bound *J–R* curve as previously was thought. This effect should be studied more extensively before any final conclusions are made. Coupling a study of constraint effects on toughness with a study of microstructural mechanisms of fracture might explain the rationale for the observed behaviour and aid with

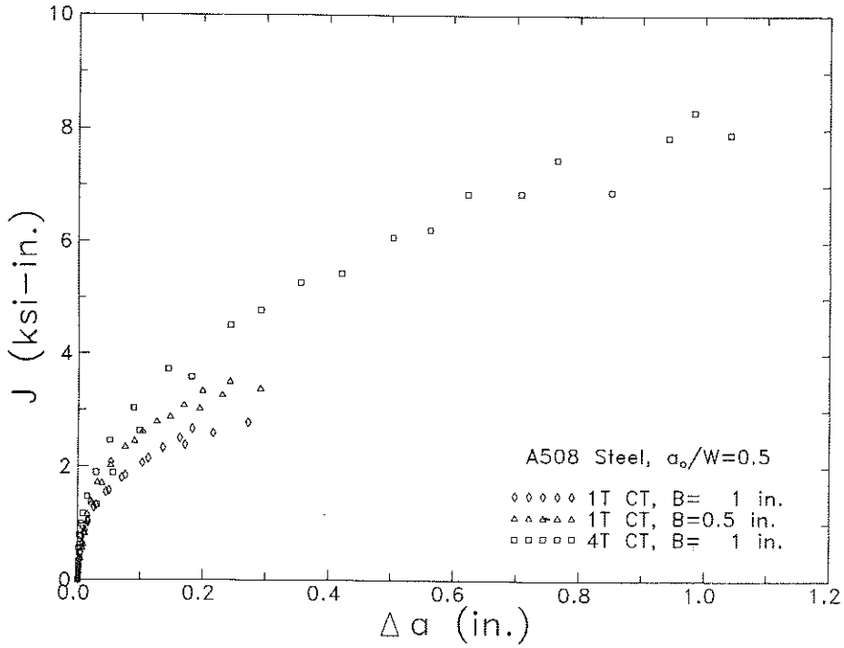

Fig 9 ***J–R* curve for A508 steel showing constraint effect**

the design of a specimen to give lower bound *J–R* curves. Such a study should be undertaken in the near future.

Conclusions

Based on the results of the experiments and analysis conducted in this study, the following conclusions are possible.

J–R curves measured using C(T) specimens were independent of specimen size for the materials investigated. Specimen size was varied up to one order of magnitude with no effect on the measured *J–R* curves. It was not necessary to use J_M to account for differences in specimen size.

Geometry effects on *J–R* curves were noted in ASTM A533B specimens. As the loading mode progressed from primarily bending to pure tension, the loss of constraint of the slip line fields led to an increase in the measured fracture toughness.

Classical effects of changing constraint by varying specimen thickness were noted in ASTM A508 steel and a 5NiCrMoV steel. Systematic reduction of the specimen thickness reduced the through-thickness constraint and led to an elevation in the measured fracture toughness. A non-classical effect was observed in ASTM A736 steel and a 304 stainless steel. For these two materials, the fracture toughness was seen to decrease with specimen size. This

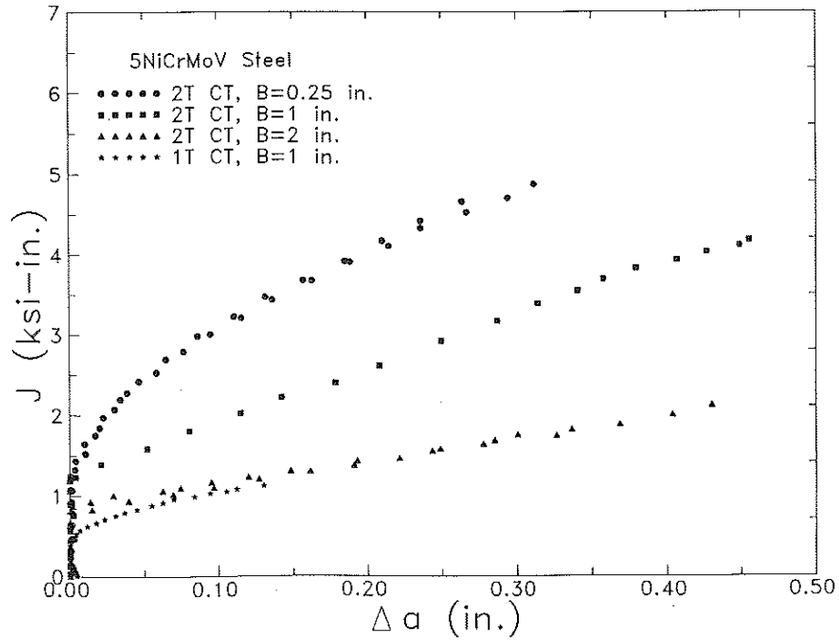

Fig 10 ***J–R* curve for 5NiCrMoV steel showing constraint effect**

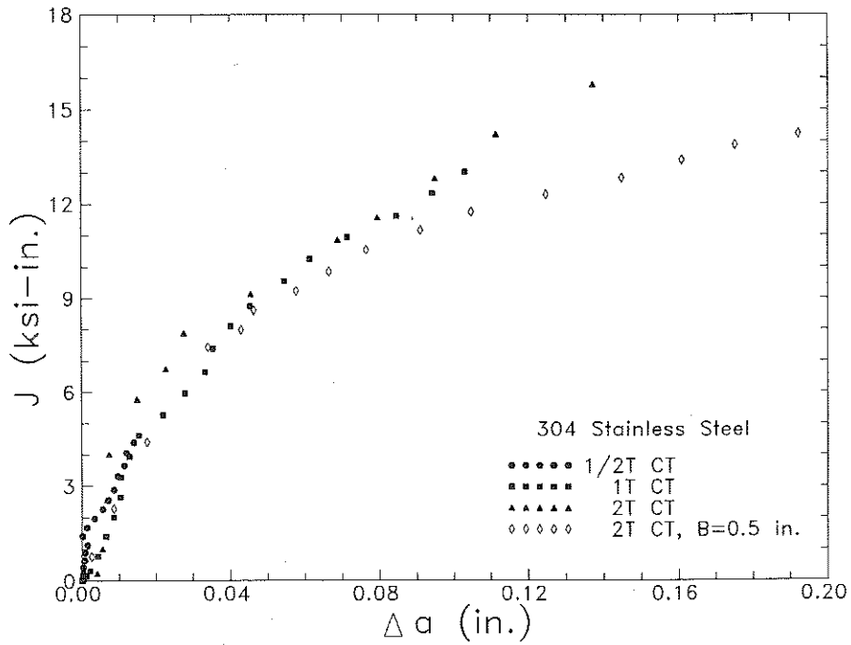

Fig 11 ***J–R* curve for 304 stainless steel showing constraint effect**

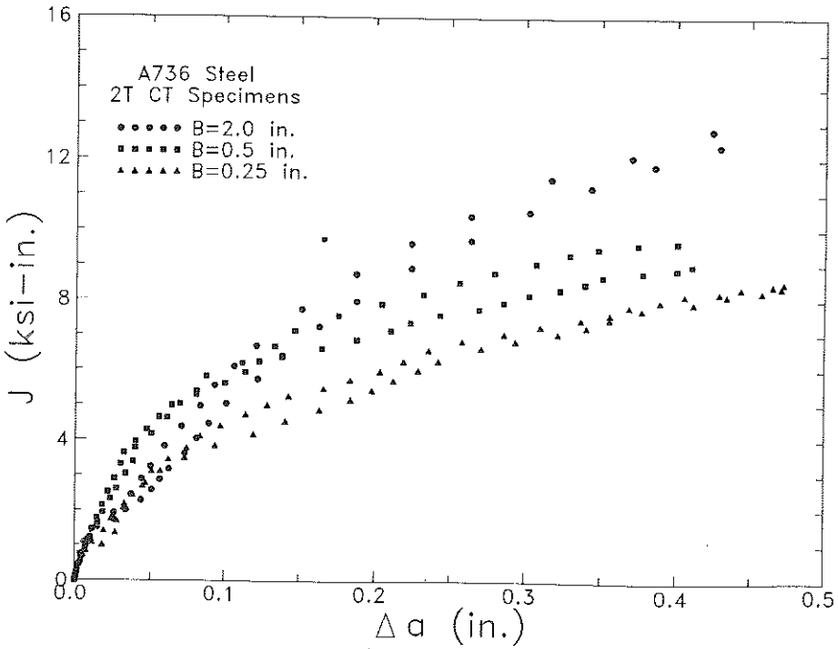

Fig 12 ***J–R* curve for A736 steel showing constraint effect**

observation is contrary to the idea that testing thick specimens leads to the development of lower bound *J–R* curves. In the future, it may be necessary to test specimens in the section size of interest in order to ensure transferability of the laboratory data to structures. Further studies of this effect are recommended.

References

(1) ERNST, H. A. and LANDES, J. D. (1986) Elastic–plastic fracture mechanics methodology using the modified *J*, *J–M* resistance curve approach, *J. Pressure Vessel Technol.*, **108**, 50–56.

(2) LINK, R. E., HERRERA, R., and LANDES, J. D. (1989) General methodology for predicting structural behavior under ductile fracture conditions, *Advances in Fracture Research*, (Proceedings of ICF-7), vol. 1, pp. 205–212.

(3) LANDES, J. D., McCABE, D. E., and ERNST, H. A. (1987) Fracture testing of ductile steels, Electric Power Research Institute Final Report NP-5014.

(4) McCABE, D. E. and LANDES, J. D. (1983) *J–R* curve testing of large compact specimens, *Elastic–Plastic Fract.: Second Symposium, Volume II – Fracture Resistance Curves and Enging Appl., ASTM STP* 803, (Edited by C. F. Shih and J. P. Gudas), ASTM, Philadelphia, pp. II-353–II-371.

(5) Standard test method for determining *J–R* curves (1987) ASTM Designation E1152-87, *Annual Book of Standards*, ASTM, Philadelphia, Vol. 03.01.

(6) SHIH, C. F., de LORENZI, H. G., and ANDREWS, W. R. (1979) Studies on crack initiation and stable crack growth, *Elastic–Plastic Fracture, ASTM STP 668*, (Edited by J. D. Landes, J. A. Begley, and G. A. Clarke), ASTM, Philadelphia, pp. 65–120.

(7) DAVIS, D. A., HAYS, R. A., HACKETT, E. H., and JOYCE, J. A. (1988) Application of the *J* integral and the modified *J* integral to cases of large crack extension and high toughness levels, presented at the 21st National Symposium on Fracture Mechanics, Annapolis, MD.

(8) LANDES, J. D. and HERRERA, R. (1989) Correcting *J–R* curve mismatch twist with normalization analysis, *Advances in Fracture Research*, (Proceedings of ICF-7), vol. 1, pp. 403–411.

(9) HERRERA, R. and LANDES, J. D. (1988) A direct *J–R* curve analysis of fracture toughness tests, *J. Testing Evaluation*, **16**, 427–449.

(10) HERRERA, R. and LANDES, J. D. (1988) Direct *J–R* curve analysis: a guide to the methodology, presented at the 21st National Symposium on Fracture Mechanics, Annapolis, MD.

(11) LANDES, J. D., McCABE, D. E., and ERNST, H. A. (1989) Geometry effects on the *R* curve, *Nonlinear Fract. Mech.: II – Elastic–Plastic Fract., ASTM STP* **995**, (Edited by J. D. Landes, A. Saxena, and J. G. Merkle), ASTM, Philadelphia, pp. 123–143.

(12) GIBSON, G. P. and DRUCE, S. G. (1989) Progress in understanding specimen size and geometry effects on ductile fracture, *Advances in Fract. Research*, (Proceedings of ICF-7), vol. 1, pp. 181–188.

(13) ERNST, H. A. (1983) Material resistance and instability beyond *J*-controlled crack growth, *Elastic–Plastic Fract.: Second Symposium, Volume I – Inelastic Analysis, ASTM* **803**, (Edited by C. F. Shih and J. P. Gudas), ASTM, Philadelphia, pp. 1-191–1-213.

(14) McMEEKING, R. M. and PARKS, D. M. (1979) On criterion for *J*-dominance of crack-tip fields in large-scale yielding, *Elastic–Plastic Fract., ASTM STP* **668**, (Edited by J. D. Landes, J. A. Begley, and G. A. Clarke), ASTM, Philadelphia, pp. 175–194.

(15) LANDES, J. D. and McCABE, D. E. (1986) Toughness of austenetic stainless steel pipe welds, Electric Power Research Institute Topical Report NP 4768.

(16) ERNST, H. A., PARIS, P. C., and LANDES, J. D. (1981) Estimation on *J*-integral and tearing modulus, T, from a single specimen test record, *Fracture Mechanics Thirteenth Conference, ASTM STP* **743**, (Edited by R. Roberts), ASTM, Philadelphia, pp. 476–502.

(17) LANDES, J. D. and HERRERA, R. (1988) A new look at *J–R* curve analysis, *Int. J. Fract.*, **36**, R9–R14.

(18) JOYCE, J. A. and HACKETT, E. M. (1989) An advanced procedure for *J–R* curve testing using a drop tower, *Nonlinear Fracture Mechanics: Volume I – Time Dependent Fracture, ASTM STP* **995**, (Edited by A. Saxena, J. D. Landes, and J. L. Bassani), ASTM, Philadelphia, pp. 298–317.

(19) LANDES, J. D. and HERRERA, R. (1988) Calculation of *J* from test records for the growing crack, *Int. J. Fracture*, **36**, R15–R20.

(20) ZHOU, Z., HERRERA, R., and LANDES, J. D. (1989) Normalization: an experimental method for developing *J–R* curves, Presented at Second Symposium on User Experience With Elastic–Plastic Fracture Test Method, ASTM, Lake Buena Vista, FL.

(21) SHAROBEAM, M. H. and LANDES, J. D., The separation criterion and methodology in ductile fracture mechanics, submitted for publication.